NASA

Technical Memorandum 84973

On the Design of an Interactive Biosphere for the GLAS General Circulation Model

Yale Mintz, Piers J. Sellers and Cort J. Willmott

January 1983

Laboratory for Atmospheric Sciences
Modeling and Simulation Facility

National Aeronautics and
Space Administration

Goddard Space Flight Center
Greenbelt, Maryland 20771

ON THE DESIGN OF AN INTERACTIVE BIOSPHERE FOR THE GLAS GENERAL CIRCULATION MODEL

by

Y. Mintz

Dept. Meteor., Univ. Maryland, College Park MD 20742, and
Lab. Atm. Sci., Code 911, NASA/Goddard Space Flight Center,
Greenbelt, MD 20771

P. J. Sellers

Resident Research Associate, National Research Council and
Hydrological Sciences Branch, Code 924,
NASA/Goddard Space Flight Center, Greenbelt, MD 20771

and

C. J. Willmott

Dept. Geography, Univ. Delaware, Newark, DE 19771.

January 1983

Table of Contents

Introduction: The need for an Interactive Biosphere in General Circulation Models.

Importance of Evapotranspiration.

The sensitivity of weather and climate to land-surface evapotranspiration is difficult to determine from observations, but has been revealed in experiments with numerical general circulation models. (See Shukla and Mintz, 1982; and the paper by Mintz, 1982, in which eleven such experiments are reviewed.) In each experiment two calculations were made, which started from the same initial atmospheric state and had the same sea surface temperatures and sea-ice extent, but with land-surface conditions that produced different evapotranspirations. In every case the result was a large difference in the calculated precipitation, temperature and motion field of the atmosphere.

A decrease in latent heat transfer from the land to the atmosphere is approximately balanced by an increase in the sensible heat transfer. The sensible heat transfer, however, warms the air within the relatively shallow planetary boundary layer, and it does so locally in space and time. The latent transfer, by contrast -- if realized as heating through the convective condensation process -- warms the air in the free atmosphere up to the tropopause level. Moreover, because of water vapor advection, the realization of the heating may be at some distant place and a later time. It is the difference in the vertical distribution of the two kinds of heating, as well as the possible shift in their horizontal distributions, which makes the general circulation (the thermally-forced large scale atmospheric circulation) sensitive to land-surface evapotranspiration.

Importance of Vegetation.

Because numerical weather predictions and predictions of climate anomalies with general circulation models will be sensitive to the land-surface evapotranspiration, great care must be used in the way in which the evapotranspiration is calculated.

In almost all existing general circulation models (see the review by Carson, 1982), an "open bucket" formulation is used to calculate the transfer of water vapor from the land to the atmosphere. The level of the water in the bucket is lowered when evaporation is larger than precipitation; and the level is raised when precipitation is larger, up to the point at which the bucket overflows and produces "runoff". Over some broad range in the level of the water in the bucket (which varies somewhat from model to model), the rate of evaporation is taken as equal to (or nearly equal to) the evaporation from a free water surface; and only when the water level is low is the evaporation rate made less than that from a free water surface. But this is hardly the way in which water vapor is transferred from the land to the atmosphere in the real world.

A more realistic representation of how water is exchanged between the land and atmosphere is shown in Fig. 1 (from Rutter, 1975). Here the atmosphere is insulated from the water in the soil by a vegetation layer; and the largest part of the water transfer to the atmosphere is the transpiration of water which the roots of the plants take up from the soil. Another large part of the precipitation (and under some vegetation and precipitation conditions the largest part) never enters the soil at all, but is intercepted by and stored on the surface of the plants and from there evaporated into the air. The third transfer process, the

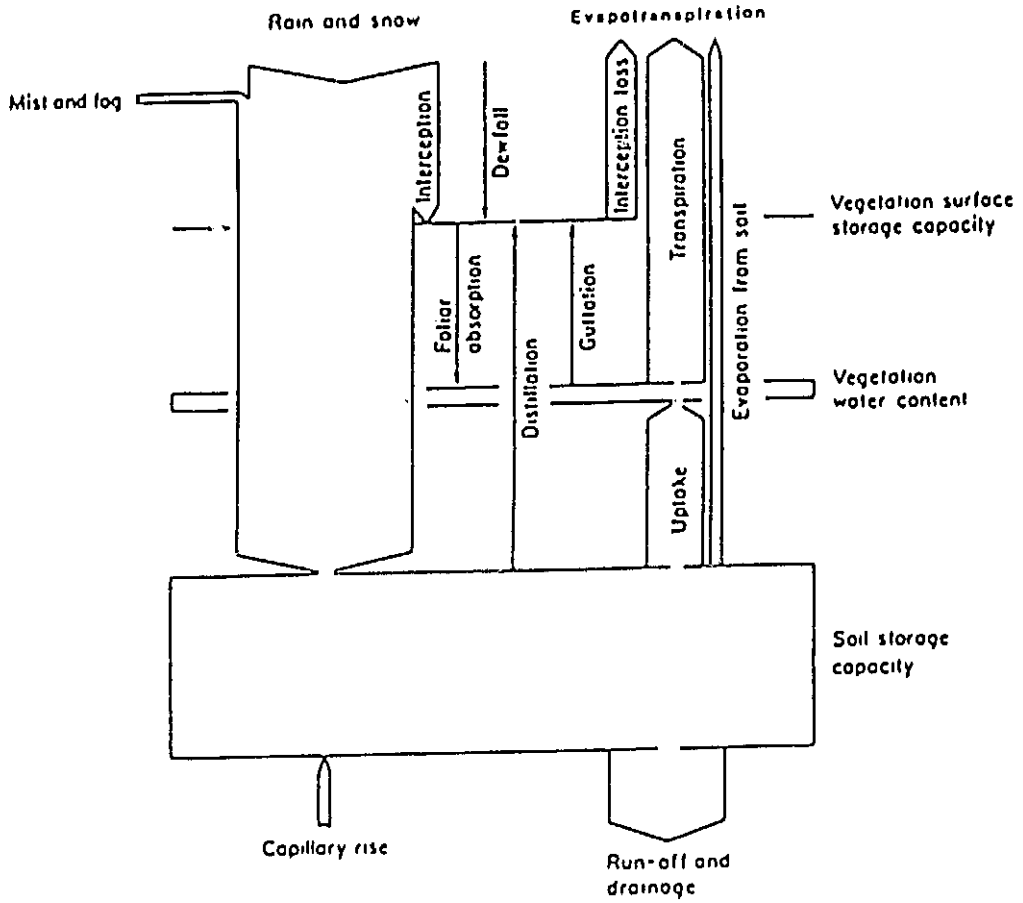

Fig. 1 Water transfers and water stores in the vegetation-soil system (after Rutter, 1975).

evaporation of water from the pores of the soil, is generally much smaller than the other two transfers.

The water storage capacities on the surface of the plants, within the plants and within the plant root zone of the soil, are of the order of 1, 10 and 100 mm, respectively. Inasmuch as both the interception loss and the transpiration are of the order of a few mm per day, the characteristic recycling time for the intercepted water is of the order of a few hours, and for the soil moisture store it is of the order of a month.

The 100 mm of water which the vegetation can remove from the soil is only a small fraction of the total water in the ground. Similarly, of the total of about 30 mm of water vapor held in an atmospheric column, only about 3 mm, out of about the 10 mm in the planetary boundary layer, can be removed from the atmosphere by the convective precipitation process. (Reducing the relative humidity in the PBL by more than about 30% shuts off the convection.) Thus, if not renewed, water vapor in the atmosphere can provide only about 1 day's worth of space-averaged convective precipitation. Soil moisture, however, even when not renewed, can maintain the average rate of evapotranspiration for about a month. It is this which makes the soil moisture store more important than the atmospheric water vapor store for numerical weather predictions and predictions of monthly and seasonal anomalies of climate.

Vegetation exerts physiological and morphological controls over evapotranspiration. Because transpiration is associated with photosynthesis, it is usually confined to the daylight hours; unlike the open bucket formulation, which can produce appreciable evaporation at night. Moreover, when water is available, the rate of the bucket evaporation is limited only

by the atmospheric factors of radiation, wind speed and air humidity; and the daytime rate, especially in semi-arid regions, can be very large. But with plants there is also a daytime limit to the transpiration rate, because there is a constraint on the rate at which water can flow through the plants.

The morphology (the vertical structure) of the vegetation has a large influence on the rate of interception loss. With tall (forest) vegetation, the elevated and dispersed surfaces of the leaves are more strongly ventilated than are the surfaces of the leaves in short (herbacious) vegetation. When the leaf surfaces are wet, therefore, the interception loss from tall vegetation is much greater than that from short vegetation. But when the leaf surfaces are dry, the greater ventilation of tall vegetation is generally compensated by its larger stomatal resistance; so that (under the same atmospheric conditions) the transpiration losses for tall and short vegetation are not very different.

The interception loss rate from short vegetation is not much larger than its transpiration rate; but with tall vegetation, the interception loss rate can be 5 to 10 times larger than the transpiration rate. Even though the vegetation surface storage capacity is small, the time-integrated interception loss from tall vegetation can be very large.

Fig. 2 is an example of the mean annual water and energy balances of short and tall vegetation, as derived from measurements in two adjacent catchments which have nearly the same atmospheric conditions. The total evapotranspiration loss from the forest catchment is more than twice as large as that from the grass-covered catchment. With the grass-cover, 58% of the net radiational heating of the surface is used for evapotranspiration, and 42% for the sensible heating of the atmospheric boundary layer. But

with the forest cover, the energy used for evapotranspiration exceeds the radiational heating by 15%, and this results in a removal of sensible heat from the boundary layer (there is a negative Bowen ratio, -0.13). In the forest case it was possible to measure the two components of the evapotranspiration separately, and the interception loss was 1.7 times larger than the transpiration. Although the atmospheric conditions are about the same for the two catchments, the net radiational heating, R_N, is about 10% larger with the forest-cover than with the grass-cover. This is not only because the forest is darker and absorbs more of the incident solar radiation, but also because, as a consequence of the larger evapotranspiration rate, the surface temperature of the forest is lower and emits less infrared radiation. It is clear, from numerous examples of this kind, that vegetation exerts a large control over the water and energy exchange between the land-surface and the atmosphere.

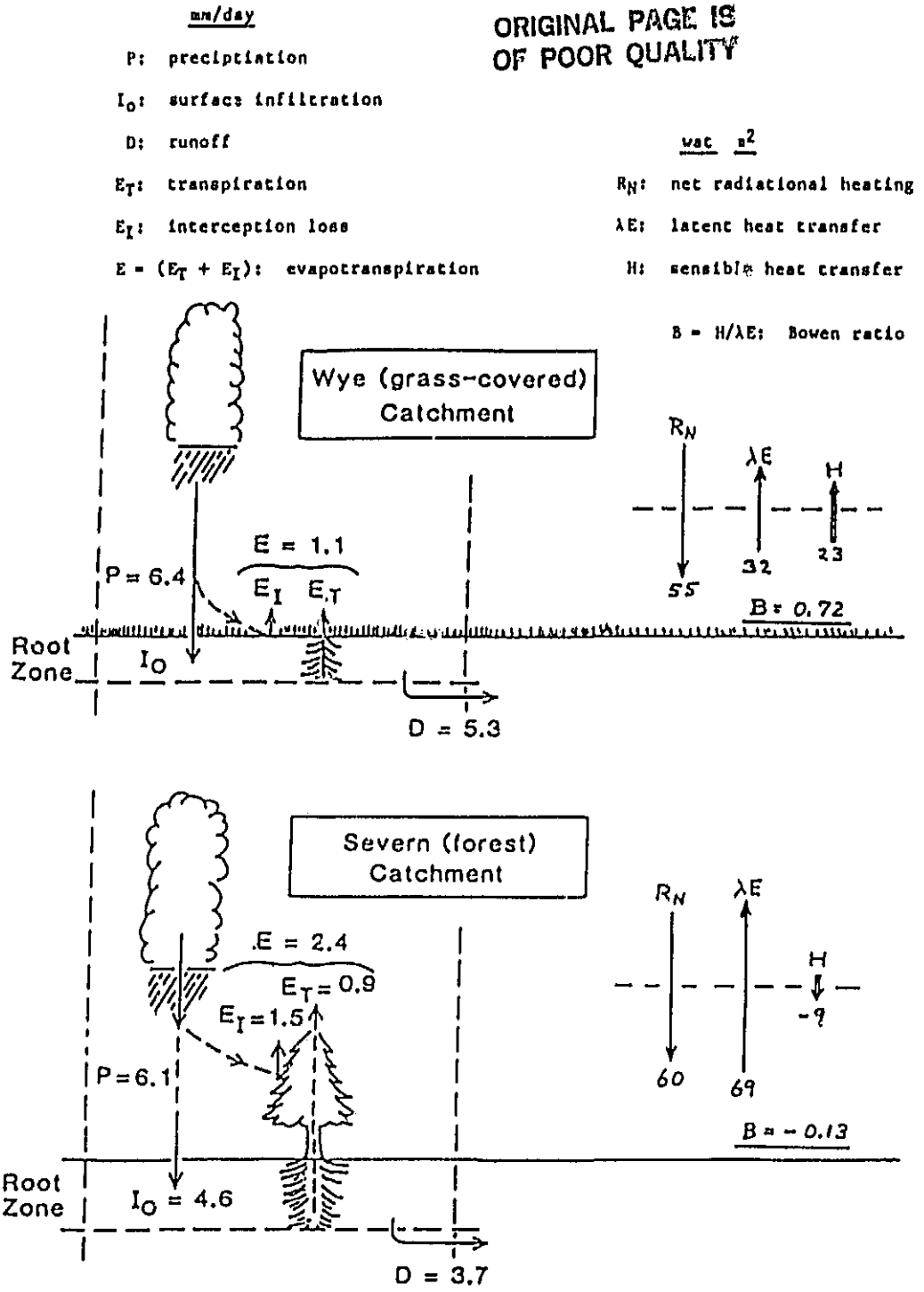

Fig. 2 Measured mean-annual water and energy balances of adjacent grass-covered and forest-covered catchments, in central Wales, U.K. (from Calder and Newson, 1979; Shuttleworth and Calder 1979).

A. Goals of the Proposed Research.

The objective of the proposed research is to construct a model biosphere which will produce realistic simulations of the water and energy transfers at the earth's surface. This will be done by constructing a numerical model of the earth's vegetation cover which embodies the principal morphological and physiological factors that control the water and energy transfers.

Morphology

The morphological factors (those which depend on the form and structure of the plants) will be the leaf area density (the total area of the leaf surfaces per unit volume of space) as a function of height, $L_D[Z]$; and the root length density (the total length of live roots per unit volume of space) as a function of depth, $RT_D(Z)$.

In the initial version of the model biosphere, $L_D[Z]$ and $RT_D[Z]$ will be prescribed for each grid area of the GCM as a function of the time of the year, as obtained from phenological observations.

In the second stage, $L_D[Z]$ and $RT_D[Z]$ will be made interactive with the model calculated atmospheric conditions (and soil moisture), so that aperiodic drought and extremes of heat and cold will also affect these two parameters on the phenological time scale.

In the final stage, the different vegetation formations themselves (i.e., rainforest, seasonal forest, woodland, desert; grassland) and not just their phenological changes will be made interactive with the atmospheric conditions (and soil moisture.)

Physiology

The principal physiological factor will be the stomatal resistance, r_{st} (the impedence to water vapor transfer from the saturated cavities within the leaves to the air outside.) r_{st} will depend not only upon the atmospheric variables, but also upon other internal resistances which affect the water flow from the soil to the leaves via the roots and stems.

B. Overview of the Proposed Biosphere.

As described in Section B.2, the vegetation of the model biosphere will have two or more discrete canopy layers and two root layers. The two important vertically continuous vegetation properties that will be discretized are $L_D[Z]$, the leaf area density as a function of height, and $RT_D[Z]$, the root length density as a function of depth.

B.1.i Governing equations for transpiration and water uptake by roots.

For the purpose of illustration, we show here the governing equations for the simple case where there is one canopy layer and one root layer.

For the definitions of the symbols, see Section C, p 39.

Transpiration:

If the vegetation is represented as a single, continuous, transpiring surface of unit area per unit ground area, the governing equations for the energy transfers can be written:

$$\lambda E_T = \frac{(e_\ell - \underline{e_a})}{(r_{st} + r_a)} \frac{\rho C_p}{\gamma} \tag{1}$$

$$e_\ell = e^* [T_\ell] \tag{2}$$

$$\frac{(T_\ell - \underline{T_a})}{r_a} \rho C_p = H \tag{3}$$

$$H = (\underline{S_a} (1-\alpha) + \underline{R_{La}} - \sigma T_\ell^4) - \lambda E_T - \underline{G} \tag{4}$$

$$r_a = r_a[L_D[Z], \underline{u_a}, (T_\ell - \underline{T_a})] \tag{5}$$

$$r_{st} = r_{st}[r_{st,o}, \underline{S_{a,o}}, \psi_{\ell,min}, \underline{RH_a}, T_\ell, L_\sigma] \tag{6}$$

Given $\underline{e_a}$, $\underline{T_a}$, $\underline{u_a}$, $\underline{S_a}$ and $\underline{R_{La}}$ from the output of the atmospheric part of the general circulation model; $\underline{G}$ from the heat budget of the soil (see section iv); and ψ_ℓ from the solution for the water uptake from the soil, as described below, we can solve these six equations for the six unknowns: E_T, e_ℓ, T_ℓ, H, r_a, r_{st}.

(1) As shown schematically in Fig. 3, the main part of the transpiration loss is water which evaporates from the walls of the mesophyll cells that surround the sub-stomatal cavities in the leaves of the plant and then diffuses to the atmosphere through the stomatal openings. [The rate of water vapor transfer across the cuticle surface of the leaves, or across other parts of the plant surfaces, is usually one to two orders of magnitude smaller.] The rate of the water vapor transfer, from its origin in the sub-stomatal cavities to a given reference level in the atmosphere, is given by Eq. 1, where e_ℓ is the vapor pressure in the sub-stomatal cavity, and $\underline{e_a}$ is the vapor pressure at the reference level in the atmospheric boundary layer. r_{st} is the bulk resistance to the diffusion of water vapor through the stomatal opening, and r_a is the resistance to the diffusion of water vapor from the vegetation surface to the reference level. With $\underline{e_a}$ given, Eq. (1) has 4 unknowns: E_T, e_ℓ, r_{st}, r_a.

(2) e_ℓ can be taken as the saturation vapor pressure, e^*, as given by the Clausius-Clapyron equation for the temperature of the leaf, T_ℓ. T_ℓ is assumed to be constant throughout the leaf (whose thickness is typically about 1 mm) and represents an additional unknown.

(3) T_ℓ is obtained from the diffusion equation for the sensible heat transfer from the surface of the leaf, at temperature T_ℓ, to the reference level in the atmosphere, at temperature, $\underline{T_a}$, where it is assumed that r_a is the same for the sensible heat diffusion as for the water vapor diffusion; which adds the unknown, H.

(4) H, the sensible heat transfer, is obtained from the total vertical energy transfer, where the sum of the three terms within the parentheses on the right, in Eq. 4, is the net radiation flux, R_N. $\underline{S_a}$ and $\underline{R_{La}}$

are the downward components of the solar and longwave radiation, as given by the atmospheric part of the GCM, α is the albedo of the vegetation surface, and σT_ℓ^4 is the upward longwave radiation, which depends on the temperature of that surface. G is the sensible heat transfer through the vegetation and into the soil, as given by the heat budget for the soil (section iv).

(5) The aerodynamic resistance, r_a, depends on the vertical distribution of the leaf area density, on the wind speed at the atmospheric reference level, and on the thermal stability of the air, $(T_\ell - T_a)$, (see, for example, Goudriaan, 1977). Typically, with wind speeds in the atmospheric boundary layer of a few meters per second and mid-day unstable lapse rates, r_a is of the order of 0.5 s cm^{-1} for herbacious vegetation (0.1 to 1 m high) and of the order of 0.05 s cm^{-1} for forests (10 to 20 m high).

(6) r_{st}, the bulk stomatal resistance reaches the minimum value for the plant species, $r_{st,o}$, when the stomates are fully open. Typically, when the leaf area index is about four, $r_{st,o}$ is of the order of 0.5 s cm^{-1} for herbacious plants, and somewhat larger, of the order of 1.0 s cm^{-1}, for trees.

The stomates close when the solar radiation, S_a, drops below a critical value $S_{a,o}$; they close when the relative humidity of the air, $RH_a = RH[e_a, T_a]$, falls below a critical value, $RH_{a,crit}$; and they close under extremes in the leaf temperature, T_ℓ. In addition, the stomates close when the water potential in the guard cells (ψ_ℓ) that surround the stomates, falls to a limiting value, $\psi_{\ell,crit}$. (What controls the magnitude of ψ_ℓ is discussed below.) When the stomates are closed, the transpiration is only through the cuticle of the leaf,

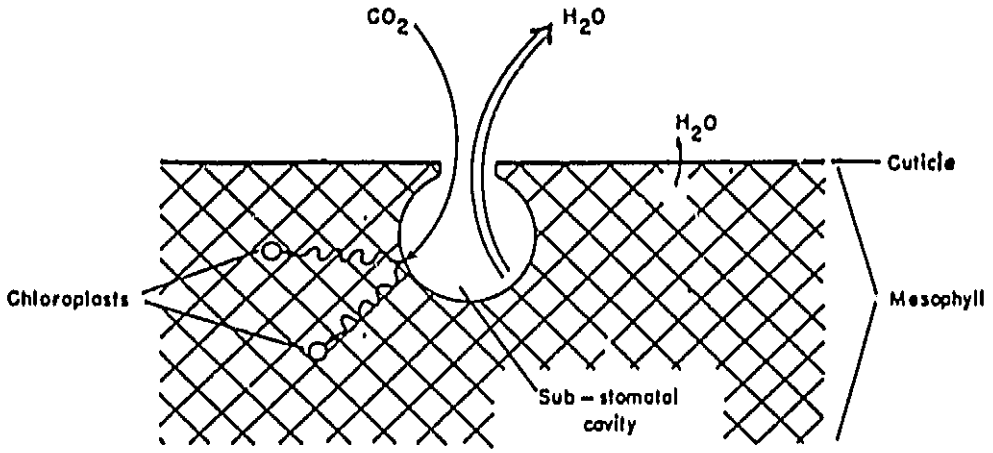

Fig. 3 Schematic representation of transpiration through the stomates and cuticle of a single leaf (after Hillel, 1971).

whose resistance to the water vapor transfer is typically about two orders of magnitude large.. than r_{st}, or about 50 to 100 s cm^{-1} when L_σ equals four.

All these responses are interpreted as the evolutionary result of the plant's effort to maximize photosynthetic production (which requires the simultaneous presence of shortwave radiation, water, carbon dioxide, and solutes in the leaf chloroplast cells), to maintain a solute transport system, to avoid heat death, and to conserve water in the soil moisture store for future use. The first three demands are in direct conflict with the last, the conservation of water, which gives rise to the need for physiologically regulating the flow of water through the plant.

Water Uptake by the Roots:

The conservation of mass requires that the water vapor which moves away from the cell walls of the sub-stomatal cavities be replaced by a flow of liquid water toward the walls on the other side.

If, for the purpose of illustration, we neglect the small time rate of change of the water stored in the plant, we have

$$E_T = F_p = U_R \quad ,$$

where E_T is the rate of transpiration, F_p is the rate of liquid water flow through the plant, and U_R is the rate of water uptake by the roots.

When there is no divergence in the water flow through the plant (no change in the plant water storage), we can write the governing equations for the rate of water flow as

$$F_p = \frac{(\psi_s - \psi_\ell)}{g(r_s + r_c + r_x)} \tag{7}$$

$$\psi_s = \psi_s[\underline{\theta}] \tag{8}$$

$$r_s = r_s[\underline{\theta},\ RT_D[Z]] \tag{9}$$

$$r_c = r_c[r_{c,o},\ RT_D[Z]] \tag{10}$$

$$r_x = r_x[r_{x,o},\ F_{p,crit}] \quad . \tag{11}$$

Given the boundary condition, $F_p = E_T$, where E_T is obtained from the solution of equations (1, 2....6) above; and given $\underline{\theta}$ from the solution for

the soil water budget (section iv), we can solve these five equations for the five unknowns: ψ_ℓ, ψ_s, r_s, r_c and r_x.

There is an upper limit to F_p, which is believed to be the rate at which the water movement through the fine channels in the xylem (the water conducting elements of the stem) changes from laminar to turbulent flow. This limit, $F_{p,crit}$, is typically of the order of 1.5 mm/hr (when expressed as the area averaged flow). When $F_{p,crit}$ is reached, there is an abrupt and large increase in the xylem resistance, r_x; and, as Eq. (7) shows, for a given soil water potential, ψ_s, this will produce an abrupt and large fall in the leaf water potential, ψ_ℓ. ψ_ℓ itself has a critical value (of the order of -25 bars) which is when which the water pressure in the stomatal guard cells can no longer maintain their turgor. When the cells collapse they constrict the stomatal opening, and $E_T = F_p$ is then limited to the value $F_{p,crit}$.

Fig. 4 is an electrical analog of the water transfer pathway through the soil-plant-atmosphere system (when $E_T = F_p = U_R$). The figure shows how the flow is controlled by the fixed resistance, r_c, and the four variable resistances, r_s, r_x, r_{st} and r_a.

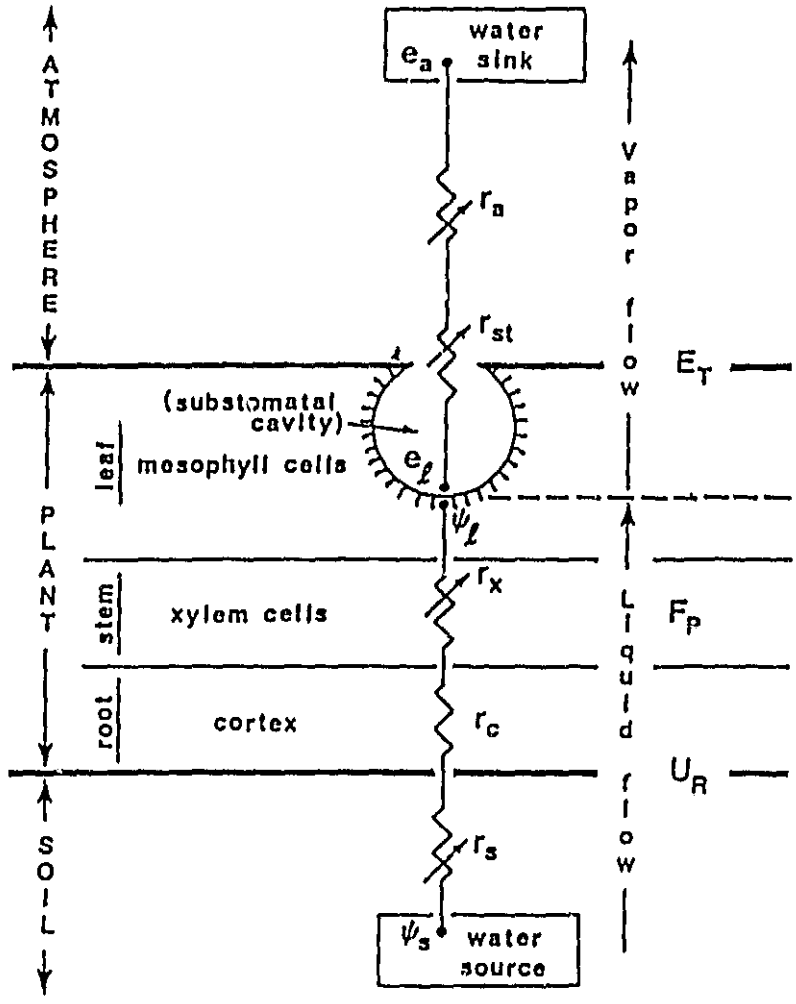

Fig. 4 Electrical analog representation of the potentials, and resistances to flow, of water vapor and liquid water in the soil-plant-atmosphere system.

ii. Rainfall Interception and Interception Loss.

For the single layer vegetation model, the governing equations for the interception loss and interception gain, when the canopy is completely wet, can be written:

$$\lambda E_I = \begin{cases} \dfrac{[e_s - e_a]}{r_a} \cdot \dfrac{\rho C_p}{\gamma} \cdot f(W_I), & \text{When } W_I > 0 \\ 0, \quad \text{when } W_I = 0 \\ \dfrac{[e_s - e_a]}{r_a} \cdot \dfrac{\rho C_p}{\gamma}, & \text{when } W_I \geq W_{I\,max} \end{cases} \qquad (12)$$

$W_{I\,max}$ is the maximum amount of water that can be held on all the upper leaf surfaces.

$$\frac{dW_I}{dt} = P\,(1 - p) - E_I - D\,[W_I] \quad . \qquad (13)$$

The interception loss and the interception gain are highly dependent on the vegetation morphology for two reasons:

i) The aerodynamic interaction between plant and atmosphere: As indicated in section B.1.i, tall, 'rough,' surfaces, like pine forests, maintain a relatively turbulent aerodynamic regime in and around their upper crowns. Within this well ventilated volume, the transfers of vapor and sensible heat are typically an order of magnitude faster than at an equivalent height above 'smoother' surfaces, like a grass cover, under the

same meteorological conditions. ($r_a \sim 0.05$ s cm^{-1} as against 0.5 s cm^{-1})

ii) The geometry and extent of intercepting surfaces: Vegetated regions commonly present 3 to 8 m^2 of surface area to the atmosphere for every square meter of ground area ($L_G \approx 3$-8). Obviously, the larger the surface area the greater the amount of rainfall that may be held on the surface for later re-evaporation, and the smaller the amount that drains off to reach the soil moisture store. Typically, the interception capacity of vegetation is of the order of 1 to 3 mm depth of water. The geometrical arrangement of the canopy is important too - some coniferous trees maintain a large intercepting surface well above the level of the theoretical momentum sink.

The rate of interception loss depends very greatly on the rainfall regime. For a given time-averaged rainfall which is made up of high intensity, short duration episodes, there will be a comparatively low rate of interception loss. This is because the interception capacity is quickly reached after the onset of storms, allowing the remaining rainfall to be transmitted to the soil surface. Conversely, if the same time-averaged rainfall is made up of long-duration, low intensity storms, the interception loss will be larger, reaching its maximum if the interception capacity is not reached (i.e. if the water does not accumulate on the leaf surfaces to a level sufficient to initiate significant leaf drainage).

As indicated in section B.2, our intention is to model the water and heat transfer processes for the several observed vegetation formation types in a realistic fashion. This, however, will produce correct values of the interception loss only if the space-time variation of the rainfall is correctly represented. General circulation models produce half-hourly to

hourly amounts of rainfall as output; but as this is the average over a large grid area (of the order of $(300\ km)^2$), if used in an unadjusted form it will almost always produce an excessively high and unrealistic interception loss. It will be necessary, therefore, to relate the GCM produced grid area average rainfall to a realistic space variation of the rainfall on the sub-grid scale, using parameters extracted from the GCM simulation (which indicates, for example, whether the rainfall is of convective or large-scale upglide origin) and also climatology. Satellite based observations of regional surface temperature and soil moisture variations (Atlas and Thiele, 1981) may be able to provide information about typical time-area-intensity distributions in the different regions and seasons, from which we would construct the area-intensity functions for the GCM rainfall calculation. A possible solution lies in representing the spatial variation of the amount of water held on the vegetation surface by wave functions. A similar wave representation of the rainfall intensity would be superimposed to obtain the spatial variation of the rate of change of the water held on the surface. Another possibility would be to assume that the rainfall at a representative point within the grid area will be equal to the grid-area averaged rainfall when both are averaged over a time interval of the order of, say, 12 to 24 hours; and then to let the half-hourly values of the rainfall intensity at that point vary within the chosen time interval as a function of the GCM parameters and climatology.

iii. Snowfall Interception and Disposal.

The partition of snow into surf ce evaporation and melt water, which contributes towards soil moisture recharge and runoff, is of great importance for the surface energy balance and hydrology of a large part of the Northern Hemisphere continents. The energy balance at the snow surface can be modelled using derivations from the equation set outlined in section B.1.i. Major differences between the fluxes of latent and sensible heat with and without snow, under the same atmospheric conditions, arise from variations in the surface albedo and hence in the net radiation, and from the value of the aerodynamic resistance, r_a. [A review paper by Male and Granger, 1981, discusses these and other facets of snow surface processes in detail.] The energy available for evaporation and/or snowmelt in forested regions is characteristically much greater than that over bare or grass covered areas (Leonard and Eschner, 1968) due to the smaller albedo of the exposed parts of the forest canopy. This produces an appreciable transfer of heat, in radiative and sensible form, from the exposed parts of the tree canopy to the snow covered surfaces. This effect is enhanced in areas with evergreen vegetation. The use of a multilayer vegetation model coupled with a layered soil model is the most realistic way to simulate the energy exchange processes involving snow cover.

iv. Water and Heat Budget of the Soil.

For simulating the water and heat budgets of the soil, we shall follow one of the more physically realistic treatments (see, for example, the reports of Gurney and Camillo, 1982, Camillo and Schmugge, 1982). In these treatments, the fluxes of heat and moisture are coupled as both depend on the gradients of temperature and moisture. This requires the simultaneous solution of the equations:

$$q_\theta = D_\theta \left(\frac{d\theta}{dz}\right) - D_T\left(\frac{dT}{dz}\right) - K_\theta$$

$$q_h = K_T\left(\frac{dT}{dz}\right) - \lambda D_{\theta,vap}\left(\frac{d\theta}{dz}\right) \qquad (14)$$

where q_θ and q_h are, respectively, the fluxes of moisture and heat; $D_{T,\theta,vap}$ is the diffusivity of heat, water, or water vapor; and $K_{T,\theta}$ is the thermal or hydraulic conductivity of soil. It should be noted that D_θ and D_T have both liquid and vapor contributions:

$$D_\theta = D_{\theta,liq} + D_{\theta,vap}$$

$$D_T = D_{T,liq} + D_{T,vap} \quad . \qquad (15)$$

Equation (14) describes the dependence of the heat fluxes on the vertical gradients of θ and T. The time dependence of θ and T is given by the continuity equations:

$$\frac{d\theta}{dt} = -\left(\frac{dq_\theta}{dz}\right)$$

$$\frac{dT}{dt} = -\frac{1}{c_s}\left(\frac{dq_h}{dz}\right) \qquad (16)$$

where c_s is the specific heat of the soil.

Various numerical techniques may be applied to solve the equation set over finite time steps. It is usual practice to prescribe a deep soil temperature and moisture content as lower boundary conditions and an energy balance model at the soil surface to calculate q_θ, q_h, θ and T at the air-soil interface. The soil is then divided into a number of strata, which are taken as internally homogenous with uniform values of $D_{\theta,T}$ and $K_{\theta,T}$. The values of T and θ for each stratum are used to calculate the depth dependent derivatives at each time step.

The soil moisture store will be represented by three zones: a small near-surface store, from which not only root uptake but also direct evaporation can take place; an intermediate bulk soil moisture store, which is mainly drawn on by the root uptake; and a deep store, from which only capillary rise can bring water toward the surface. The last term can be significant on the seasonal time scale.

The hydraulic and thermal properties of the soil will be taken from the global data set prepared for the GLAS GCM by Lin and Alfano (Alfano, 1981).

It is impossible to model overland flow and soil interflow, in a direct way, without resort to an exceedingly fine grid size. Instead, we will use the 'lumped' catchment analytical model of Beven and Kirkby (1976). This makes use of functions which relate the total soil moisture storage to the size of the catchment contributing area, (which is the saturated area bordering stream channels), thus allowing a direct calculation of the different components of runoff: overland flow, interflow and base flow. It may be possible to use the geographical data relating to grid square soil type, topography and stream density to parameterize the necessary functions.

B.2 The Multilayer Vegetation Model.

1) Definition and Advantages of a Multilevel Model.

Definition:

In general, a multilayer model can be thought of as an elaborate extension of the short set of equations given in Section B.1.i. The vegetation canopy is represented by a vertical series of discrete plates, each of which exchanges sensible and latent heat with the immediately surrounding air and through which the fluxes must pass on the way to the free atmosphere (see Fig. 5). At the same time, the temperature of each plate depends on the net radiation it absorbs (which is a function of the temperatures of all the plates and the soil surface), and on the temperature and vapor pressure of the air in the surrounding (canopy) air space. It is apparent from Figure 5 that, given: (1) the air temperature (T_a) and vapor pressure (e_a) above the canopy, and their equivalents below the soil surface; (2) the values of the intermediate resistances and (3) a means of distributing the shortwave and downward longwave radiation among the plates, the equation set representing the energy budgets of all plates will reduce to n expressions with n unknowns, (where n is the number of leaf layer plates and the unknowns are the leaf temperatures.) A similar model will represent the layers of the soil. The combined system will represent the steady state energy balance of the vegetation and soil, and may be further extended to include non-steady state processes - such as the drying out of intercepted water which involve a dependence on the time variation of canopy and soil temperatures and water contents.

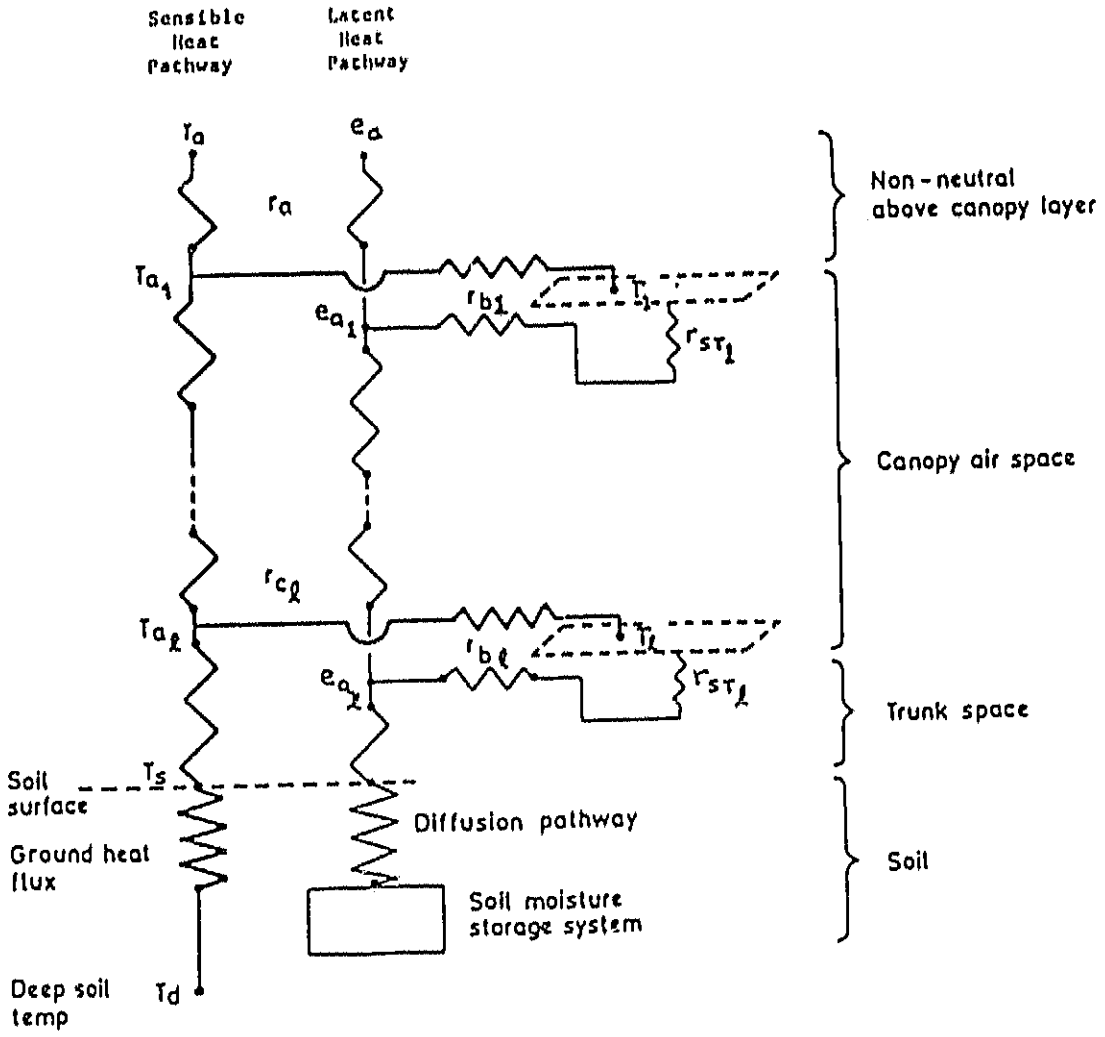

Fig. 5 Schematic representation of sensible and latent heat transfer using a multilayer model. The flow of water from soil to leaf layers has been omitted for clarity.

T_a	air temperature at reference height.
e_a	vapor pressure at reference height.
T_{at}	air temperature of canopy air space of t^{th} layer.
e_{at}	vapor pressure of canopy air space of t^{th} layer.
T_t	leaf surface temperature of t^{th} layer.
T_s	soil surface temperature.
T_d	deep soil temperature
r_a	aerodynamic resistance from reference height to canopy top.
r_{ct}	aerodynamic resistance between canopy air space of the t^{th} layer and the canopy air space of the $t-1^{th}$ layer.
r_{bt}	aerodynamic resistance between leaf surface and canopy air space of t^{th} layer.
r_{stt}	stomatal resistance of t^{th} layer.

Advantages:

The multilayer model is more realistic and is easier to validate than a unilayer model. The principal points to note are:

a) Vegetation morphology: A multilayer model can be constructed in such a way that the leaf area density, $L_D[Z]$, and the leaf area index, L_σ, are directly represented by the size and spacing of the leaf layer 'plates'.

b) Energy exchange processes: The exchanges of energy (in radiative, sensible and latent form) between the different layers of canopy, and between those layers and the soil, can be modelled. It need not be assumed that the multiple latent and sensible heat sources correspond to the momentum sink, as with a unilayer model.

c) Parameter correspondence with nature: The parameters of the model can be made to correspond directly to the physical and physiological properties of each vegetation type.

d) Interception loss and snowmelt: These processes cannot be modeled realistically using a unilayer treatment. Sellers (1981) demonstrated that a single-layer model consistently underestimates the rate of interception loss.

e) Validation: A multilayer model not only generates the latent and sensible heat fluxes, but also profiles of leaf temperature, air temperature, vapor pressure, soil temperature, and soil moisture potential. By comparison, the unilayer model outputs a single value of 'surface' temperature - a rather nebulous quantity when considering

that a tropical rainforest has been observed to have a mid-afternoon temperature difference of as much as 7° C between the top of the canopy and the soil surface (Pinker, 1980; and personal communication, 1982).

ii. Distribution of the Observed Vegetation Formations.

de Laubenfels (1975) has made the following classification of the earth's vegetation formations, whose distributions are shown in Fig. 6:

Region with tall trees whose crowns form a continuous canopy, and below which there is a continuous understory of shorter trees: designated Rainforest.

Region with trees whose crowns form a continuous canopy, but below which there is a discontinuous understory: designated Seasonal Forest.

Region with trees whose crowns do not form a continuous canopy, but where the total vegetation cover is continuous: designated Woodland.

Region where there is a discontinuous cover of plant growth, so that large areas of bare ground are exposed: designated Desert.

Region of continuous ground cover of herbacious plants (of which grass is the predominant form): designated Grassland.

Rainforest, Seasonal Forest, Woodland, and Desert are "undisturbed" vegetation formations. Grassland is the existing formation type where seasonal forest and woodland have been disturbed by fire and by grazing (which inhibits recovery after fire.)

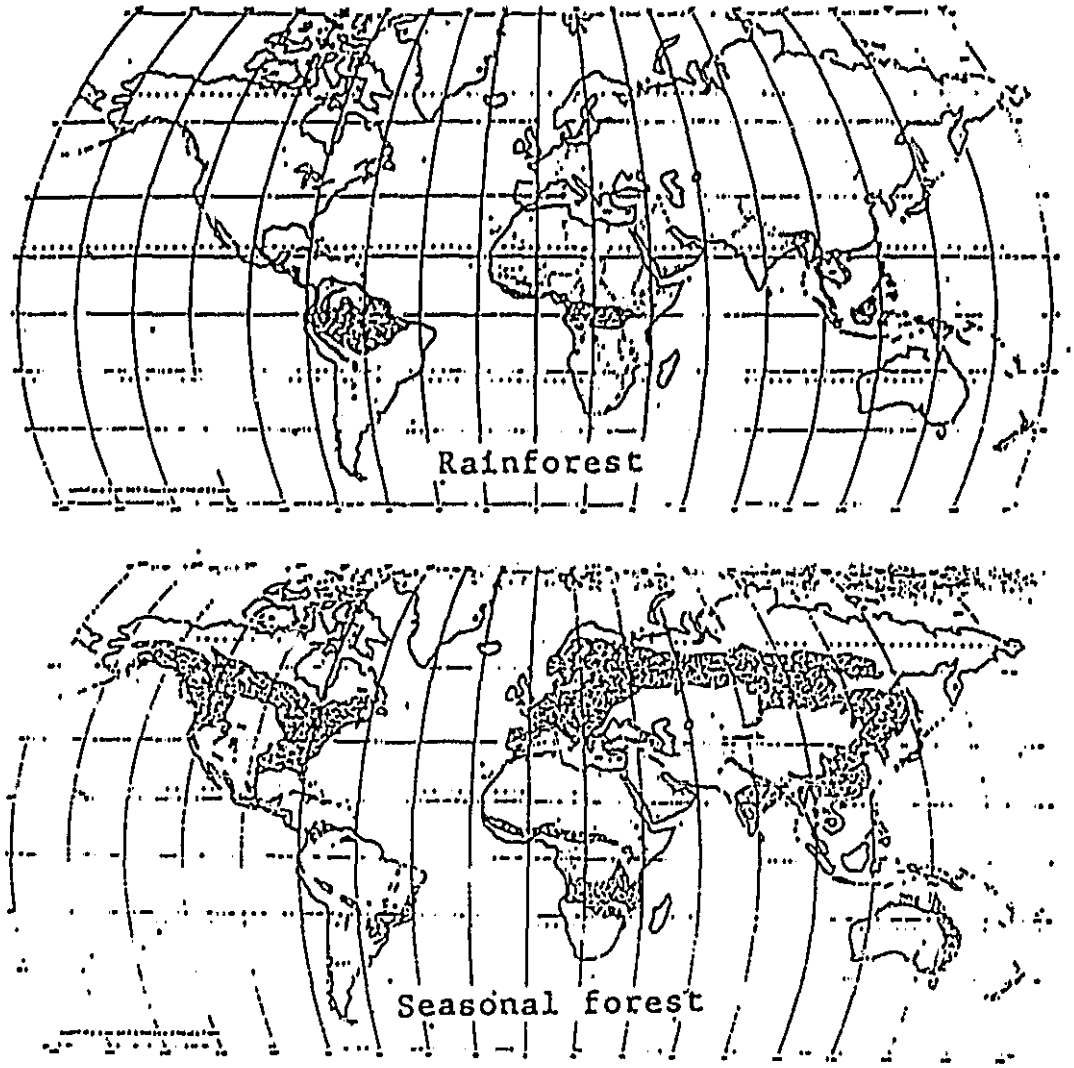

Fig. 6 Observed vegetation formations (from de Laubenfels, 1975).

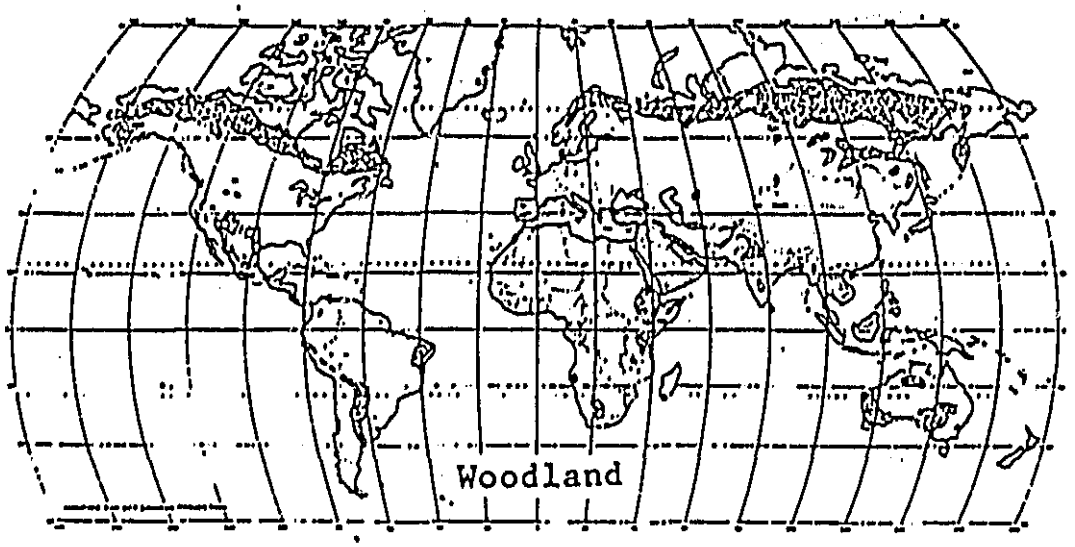

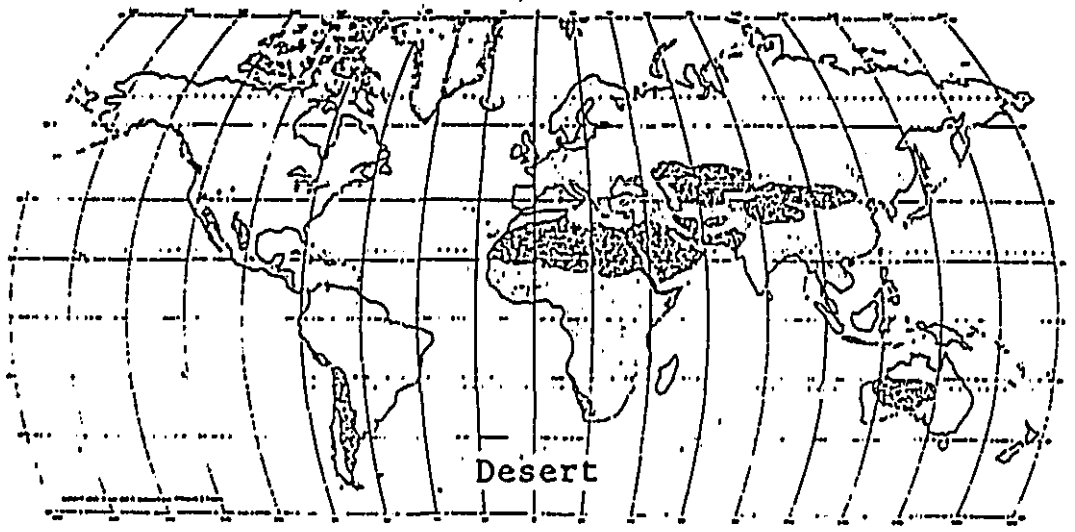

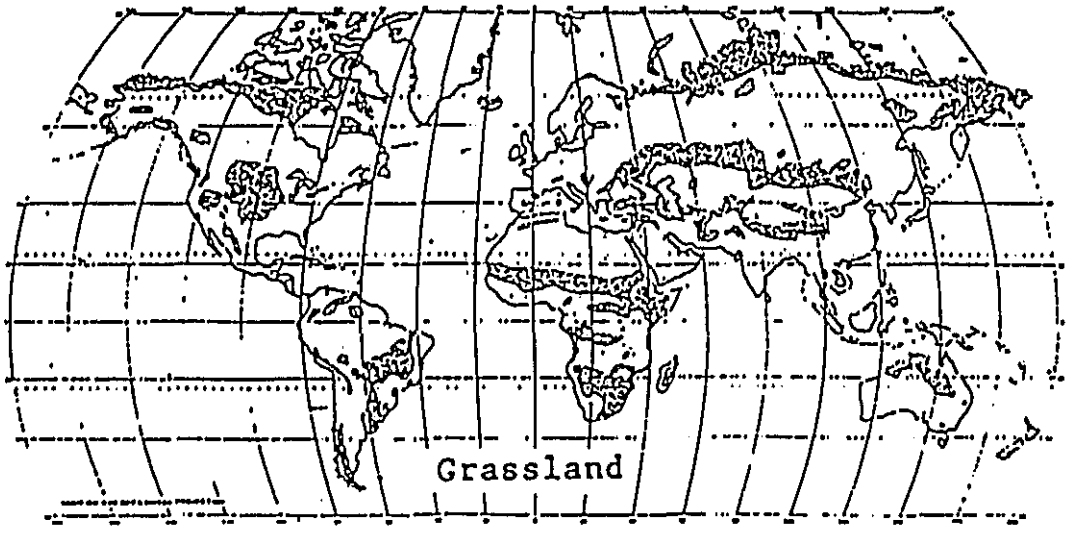

Fig. 6 - continued.

In the initial version of the proposed biosphere, the prescribed distribution of the vegetation formations will not change with time.

Eventually, we would like to have the vegetation formations change in response to forcing by the atmospheric part of the GCM. But inasmuch as the time scale of natural succession is of the order of 10^1 to 10^3 years (see, for example, Loucks, et. al., 1981) this will be an essential requirement for the biosphere only when a fully interactive ocean is made part of the general circulation model.

iii) Specification of the Multilayer Model.

There are two distinct requirements for the specification of the multilayer model. Firstly; the morphology of the vegetation community must be realistically represented by the size and spacing of the discretized leaf plates (see Fig. 5), and by the values of the boundary layer resistances, canopy air space resistances and root cortex resistances. The above canopy aerodynamic resistance, r_a, must also be properly related to the gross morphology of the vegetation community. Secondly; the physiology of the plant must be correctly reflected in the functional model of stomatal response and its interaction with the leaf water potential, xylem resistance, stem flow, and soil moisture potential.

Taking the morphology of the vegetation community first: Figs. 7A, B, C illustrate the process whereby measurable characteristics of the vegetation are transformed to model parameters. Fig. 7A shows the structure of a tropical rain forest in its natural state. Fig. 7B shows the corresponding leaf area density and root length density as functions of height. In the first version of the model, the seasonal variations in these vegetation parameters will be prescribed as functions of the time of the year. Later, the phenolgical changes in $L_D(Z)$ and $RT_D(Z)$ will be made dependent upon the model derived atmospheric variables and soil moisture.

To obtain the areas of the two plates that will represent the vegetation (see figure 7C), the leaf area density is integrated with height:

$$L_\sigma = \int_{Z_B}^{Z_T} L_D(Z) \cdot dZ \qquad (17)$$

where L_σ is the leaf area index (m^2/m^2), and Z_B and Z_T are the heights of the bottom and top of the storey.

Abstract

The purpose of adding an interactive biosphere to the GLAS general circulation model is to make the calculation of land-surface evapotranspiration and sensible heat flux more realistic and, therefore, more accurate. This is important because sensitivity experiments with general circulation models have shown that the large scale fields of rainfall, temperature and motion of the atmosphere are highly sensitive to the transfers of latent and sensible heat at the land surface.

Water and energy transfers at the land surface depend on vegetation morphology and physiology. In the proposed model biosphere, the vegetation morphology will control these transfers through the leaf area density as a function of height, $L_D(Z)$, and through the root length density as a function of depth, $RT_D(Z)$, as expressed in a discretized form for each of the model grid areas. $L_D(Z)$ will influence (a) the aerodynamic resistance to the latent and sensible heat transfers; (b) the transmission, absorption and emission of radiation energy by the canopy and underlying ground; and (c) the interception, evaporation and throughfall of rain and snow. The vegetation physiology will control the transfers of water and energy through the stomatal resistance, the xylem resistance of the stems, and the root cortex resistance. The stomatal resistance will be a function of the leaf water potential, short-wave radiation intensity, leaf temperature, and humidity of the air.

In the initial formulation, $L_D(Z)$ and $RT_D(Z)$ will be prescribed as functions of latitude and longitude and the season of the year, as known from ecological observations in the various vegetation formations. Later, the phenological changes of $L_D(Z)$ and $RT_D(Z)$ in the deciduous forests and grasslands will be made interactive with the atmospheric variables and the soil moisture as calculated by the GCM. Finally, the vegetation formations themselves will be made interactive with the atmospheric and soil moisture conditions.

The realism of the model biosphere will be evaluated (1) through short period one-dimensional comparisons with measured values of the local atmospheric forcing and measured values of the vertical fluxes of water and energy; (2) through long period comparisons of simulated and observed catchment water budgets; and (3) through comparisons of the simulated and observed surface temperatures, surface albedos, snow cover, live biomass, and the water balances of the large river basins, when the model biosphere is forced with atmospheric variables taken from the FGGE level 3-B and 2-C data sets.

The height of the plate is taken as the center of gravity of the plate, Z_m, where:

$$\int_{Z_B}^{Z_m} L_D(Z) \cdot dZ = \int_{Z_m}^{Z_T} L_D(Z) \cdot dZ \qquad (18)$$

Following the work of Goudriaan (1977), the bulk aerodynamic parameters of roughness length (Z_o) and zero plane displacement (d) may be determined from a numerical analysis of the reduction in shear stress with depth in the canopy; parameters which depend on the leaf area density and drag coefficient of leaf elements. The parameters z_o and d are used to determine the value of r_a, the above canopy resistance, by

$$r_{a\ h\ z_d} = \left[\frac{\ln \left[\frac{z - d}{z_o} \right]^2}{k^2 u} \right]_h^{z_d} \qquad (19)$$

where k is von Karman's constant, h is the height of the crop and z_d is the reference height (This equation holds for neutral conditions only; but Thom and Oliver (1977) describe a version which accounts for the effect of non-neutrality). A further analysis by Goudriaan (1977) provides the extinction of wind speed as a function of leaf area density.

The conductivity of mass, heat and momentum in the canopy air space is given as:

$$K_{m,v,h_{(z)}} = L_{m_{(z)}} \cdot I_{m_{(z)}} \cdot u_{(z)} \qquad (20)$$

where L_m is the local mixing length of the canopy air space (a function of the size and spacing of shoot elements) and I_m is the relative turbulence

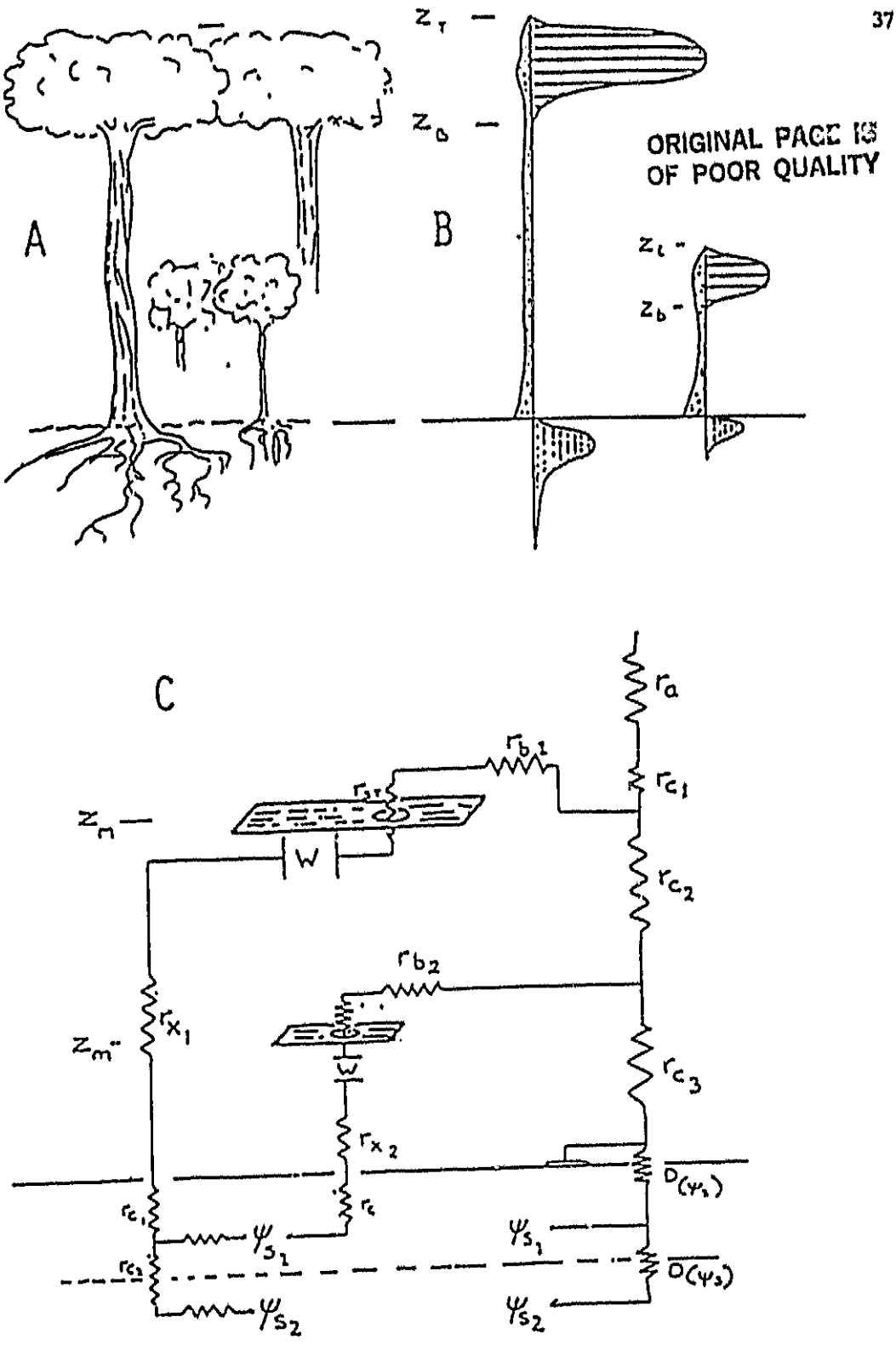

Fig. 7: A. Tropical rainforest vegetation; continuous canopy of tall trees above continuous under-storey.

B. Leaf area density ▤, stem area density ▦, and root length density ▥, as functions of height for the tropical rainforest shown in Figure A.

C. Electrical resistance analogue of the tropical rainforest represented in Figure B.

intensity - a factor that increases from 0.3 at the top of plant canopies to 0.8 at the base, and appears to be invariant with wind speed.

r_{c_ℓ}, the canopy air space resistance between one leaf layer and the next is given by:

$$r_{c_\ell} = \int_{Z_\ell}^{Z_{\ell-1}} \frac{1}{K_{m,v,h_{(z)}}} \cdot dZ \qquad (21)$$

The leaf laminar boundary layer resistance, r_{b_ℓ}, will be taken as a function of leaf area index, local wind speed, and a shape/shelter factor, χ_s:

$$r_{b_\ell} = f(L_{\sigma_{(z)}} \cdot u_{(z)} \cdot \chi_s) \qquad (22)$$

Several researchers, notably Goudriaan (1977) and Allen and Lemon (1976), have proposed different mathematical analyses to determine χ_s as a function of leaf size, shape and orientation.

The radiation absorption and transfer characteristics of the vegetation are determined by the canopy structure. A simple model of radiative transfer was proposed by Ross and Nilson (1971):

$$S_{a_{(L_\sigma)}} = S_{a_{[0]}}[f(w) + \exp(-f(\beta) \cdot L_\sigma)] \qquad (23)$$

where $S_{a_{(L_\sigma)}}$ is the shortwave radiation flux emerging from under a cumulative leaf area index L_σ, $S_{a_{[0]}}$ is the radiation intensity above the canopy, $f(w)$ is a scattering function, and $f(\beta)$ is an extinction coefficient that varies with the solar angle, β.

The root water uptake models of Cowan (1965), Hillel (1977) and others describe the movement of water from soil to root cortex as a radial flow towards individual root elements across a gradient of moisture potential - the difference between ψ_s, the soil water potential, and ψ_r, the root water potential. The plant parameter of importance is $RT_D[Z]$, the root length density ($m\ m^{-3}$), as a function of depth. Cowan (1965) originally proposed the expression:

$$\frac{\partial \psi_s}{\partial t} = \frac{D}{r} \frac{\partial}{\partial r} \left(r \frac{\partial \psi_s}{\partial r} \right) \qquad (24)$$

where D is the value of soil moisture diffusivity, and r is the distance from the root. Given that the roots have a typical radius of r_1 and that a root extracts water from a cylindrical volume of soil of radius r_2, where $r_2 = [1 / \pi . RT_D[Z]]^{1/2}$, equation (24) can be solved with the boundary conditions of

$$\frac{\delta \psi_s}{\delta r} = \begin{cases} \dfrac{d\theta}{dt} \dfrac{[r_2^2 - r_1^2]}{2r_1} & \text{at } r = r_1 \\ 0 & \text{at } r = r_2 \end{cases}$$

where dW_s/dt is the rate of reduction of soil water concentration.

The transfer of water from root cortex to leaf mesophyll involves aspects of plant morphology and physiology. The xylem elements, which conduct water up the stem are serially linked, elongated plant cells with narrow apertures at their end-to-end junctions. Poiseuille analyses of the flow in such elements (see, for example, Denmead, 1976) predicts a critical

flow velocity above which the flow regime changes from laminar to turbulent. This greatly increases the resistance imposed by the xylem and has the effect of lowering ψ_ℓ.

The end of the liquid transfer pathway is the leaf mesophyll cell. The leaf water content, W_ℓ, is determined by:

$$\frac{dW_\ell}{dt} = \frac{1}{g}\left[\frac{\psi_\ell - \psi_r}{r_c + r_x}\right] - E_T$$

Leaf water potential, ψ_ℓ, a critical variable in the calculation of stomatal resistance, is a function of W_ℓ,

$$\psi_\ell = f(W_\ell) \quad .$$

The particular form of stomatal response is dependent upon plant species, where each species can be thought of as being near perfectly adapted to survive in its natural environment. In the main, stomatal response is a function of shortwave radiation intensity, leaf water potential, vapor pressure, temperature and leaf age. Closure of the guard cells is brought about by a reduction in their turgor; this may be induced by a slow hydropassive process, whereby water is abstracted from the guard cells by strictly physical processes - such as evaporation or osmotic flow - or by a fast hydroactive process. It is believed that the latter, which can cause complete stomatal closure within seconds, is controlled by the transport and metabolism of ions into and out of the guard cells under the control of a plant hormone, Abscissic acid (ABA). The local concentration of ABA is determined by ψ_ℓ (see figure 8).

It is not proposed to model the biochemical and detailed biophysical responses of the leaf, although this has been done by some researchers

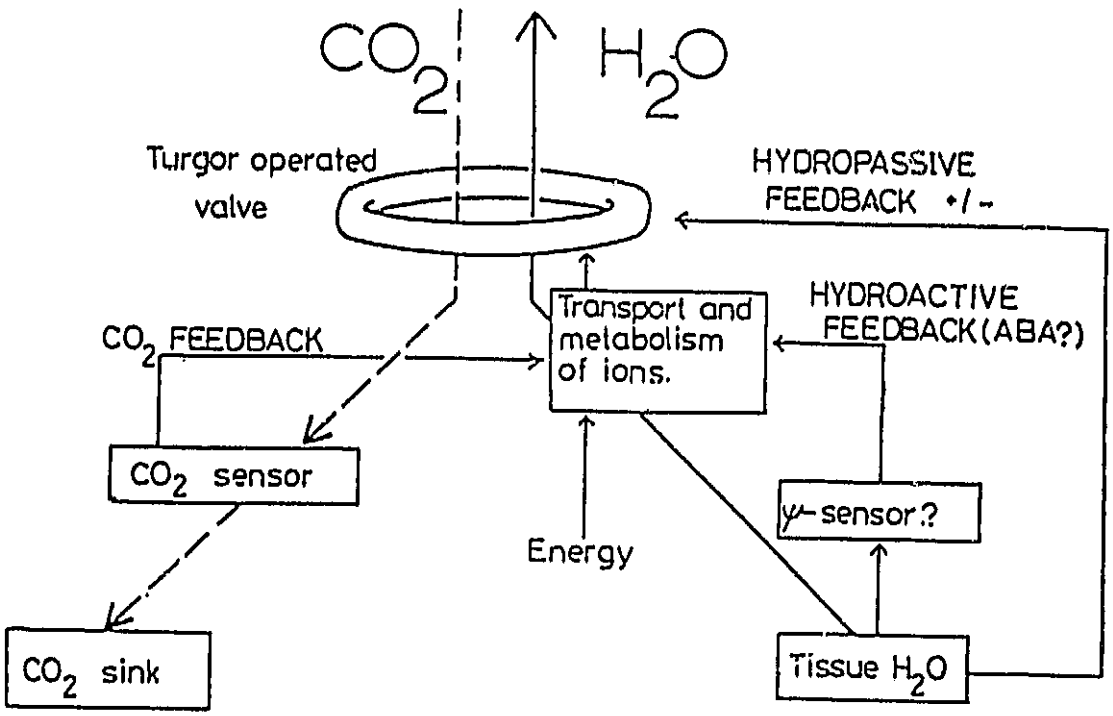

Fig. 8 Dependence of r_{st} on ψ_l and CO_2 concentration (From Raschke, 1975)

(see, for example the report of Penning de Vries; 1971); but rather to make the stomatal resistance a function of the leaf water potential and atmospheric forcing. Thus:

$$r_{st} = \frac{r_{st}(\underline{S_a})}{f(\psi_\ell) \cdot f(\underline{e_a}) \cdot f(\underline{T_a})} \tag{25}$$

Examples of the individual functions in equation (25) are given below.

Light

$$r_{st}(\underline{S_a}) = A_1/(A_2 - A_3 \cdot \underline{S_a}) \tag{26}$$

Denmead and Millar (1976)

where A_n is a species dependent constant.

Leaf water potential

$$f(\psi_\ell) = 1 - \exp(-A_4 \cdot \delta\psi_\ell)$$

$$\delta\psi_\ell = \psi_\ell - \psi_{\ell,crit} \tag{27}$$

$$0 < f_{(\psi_\ell)} < 1 \qquad \text{Turner (1974).}$$

where $\psi_{\ell,crit}$ is the value of ψ_ℓ below which the stomata close completely.

Vapor pressure

$$f_{(\underline{e_a})} = 1/[1 - A_5 (e^*[\underline{T_a}] - \underline{e_a})]$$

$$0 < f_{(\underline{e_a})} < 1 \tag{28}$$

Jarvis (1976)

Temperature

$$f(\underline{T_a}) = A_6(\underline{T_a} - T_b)(T_u - \underline{T_a})^{A7}$$

$$A_6 = 1/(T_o - T_b)(T_u - T_o)^{A7}$$

$$A_7 = (T_u - T_o)/(T_o - T_b) \qquad (29)$$

$$0 < f(\underline{T_a}) < 1$$

Jarvis (1976)

where, T_b and T_u are the temperatures above which and below which the stomata open, and T_o is the temperature at which $f(\underline{T_a}) = 1$.

B.3 Comparisons of the Model Performance with Observations.

The checking of the model's performance will be done in three phases, each of which corresponds to a further level of horizontal integration. These are briefly stated below, starting at the lowest level of integration.

i) Field Measurements.

The complete vegetation-soil model for each vegetation type will be driven offline using local micrometeorological data. There are a number of case studies reported in the literature where a short time series of simultaneous observations were made of heat and vapor fluxes, temperature and humidity profiles, and micrometeorological conditions above the canopy. Use of these data sets should ensure that the characteristics of the various vegetation types are transformed to the model in a physically reasonable way.

ii) Water Balances in Catchments.

Here, the comparisons are made over a time period of a year or more for an area where long records of meteorological and streamflow observations exist. This will allow a checking of the simulated water balance components against the observations for the different vegetation types. It should be noted that in both (i) and (ii), no allowance is made for horizontal differences in meteorological conditions: the tests are essentially one-dimensional.

iii) FGGE Observations for the Globe.

Using a 4-dimensional dynamic assimilation of ground based and satellite based observations of the atmosphere during the FGGE year (1979), the GLAS GCM is producing a time series of the atmospheric state variables, $\underline{T_a}$, $\underline{e_a}$ and $\underline{u_a}$; and of the radiation transfers $\underline{S_a}$ and $\underline{R_{La}}$, averaged for the model grid areas and at half-hourly time intervals. In addition, the GLAS model generates grid-area averaged rainfall, [P]; which will be converted into representative hourly local rainfall intensities, as indicated in section B.1.ii. The observed daily precipitation at 30,000 stations are available on tape for the FGGE year, and can also be used for input (10,000 of these are in the U.S. and have hourly records.)

This information will be used to force the model biosphere and, thereby, obtain a time series of the global fields of E_I, E_T, H, and σTs^4; W_I and W_S; and of the drainage, D_S; for the FGGE year.

The model derived σT_s^4, and its spatial and temporal variation as a function of W_I, snow cover, etc., (where T_s is the radiation temperture of the earth's surface) can be compared with satellite measurements of T_s. This will provide a quantitative evaluation.

E_T can be compared with the observed distribution of actively growing vegetation. C. J. Tucker has shown that growing and dying herbacious vegetation can be determined from Landsat observations. This, however, can only be a qualitative evaluation.

E_I, H and W_I will be difficult to evaluate. $W_{s,1}$, the moisture in the upper root zone, whose depth is of the order of 10 cm, may perhaps be compared with satellite microwave measurements of the moisture in the uppermost 5-15 cm of the soil in the desert and grassland regions (Schmugge, et.al., 1980).

D_s can be compared with the measured river flows during 1979, which are now being documented, on tape, as part of the FGGE Level 2-B data set.

•• It is the above (phenologically interactive) version of the biosphere that should be used when making weather predictions and predictions of monthly and seasonal climate anomalies with the general circulation model.

B.4 Numerical Simulation of the Vegetation Formations.

In the biosphere described above, the phenological changes of the vegetation formations will be interactive with the atmosphere and soil moisture, but the vegetation formations themselves will be prescribed (as in Figs. 6 A-E).

If the above goal of biosphere modeling is successfully accomplished by the beginning or early part of the third year, we shall undertake the next step: which is to model and simulate interactive vegetation formations. Here we will use empirical expressions which relate the climax vegetation type to the atmospheric and soil moisture conditions and thereby (starting from some initial state of the earth's vegetation cover) derive the distribution of the "undisturbed" vegetation formations: the forests, woodlands and deserts. Replacement by grassland would occur wherever atmospheric and soil moisture conditions make the forest and woodland vegetation tinder-dry: the assumption being that some mechanism for setting the dry vegetation on fire (lightning, dewdrops acting as burning lenses, or incendiary man) is always present.

A substantial extension of the above procedure would be to make use of the ecological processes which govern the growth, aging and succession of vegetation types. Starting from a given initial state, we would calculate the long term changes in the vegetation formation parameters.

Validation

Validation can be made, on the simplest non-trivial level, by forcing the biosphere with the non-interactive FGGE atmospheric data set. Here, we would assume that this one year data set represents the climate that produced the observed vegetation formations.

A higher level of validation would be to initalize the vegetation formations with the FGGE data set and then let the model atmosphere and biosphere operate in the interactive mode (with some large compression of the successional time scale.) In doing this, the presently observed ocean surface temperatures would be prescribed. Where the simulated and observed vegetation formations agreed, the model would be taken as being correct: where they disagree, we would conclude that either the model was not correctly formulated or that the presently observed vegetation formation is not in its natural equilibrium state.

Applications.

Atmosphere-biosphere fully interactive: ocean surface temperatures prescribed.

Besides the second level of validation indicated above, there will be relatively few uses for a fully interactive atmosphere-biosphere GCM when the ocean surface temperatures are prescribed (or when the ocean temperature is prognostic only in its thin boundary layer.) With given ocean temperatures, we are limited to the CLIMAP type of calculation. For example, we can prescribe the paleontologically derived global ocean surface temperatures of 18,000 years ago, and derive both the atmospheric state and the vegetation formations of 18,000 years ago.

Ocean-atmosphere-biosphere fully interactive.

Eventually we shall have a global ocean model which is fully interactive with the atmosphere and which correctly simulates the heat transport and heat storage in the deep ocean. (For a review of the near-current state of the art of ocean modelling, see Mintz, 1979.) When that is in hand, there will

be many interesting and important climate simulation and sensitivity experiments that can be made with the fully interactive ocean-atmosphere-biosphere GCM; some concerning natural variations in climate, others concerning anthropomorphic influences on climate.

An example, in the first category, would be the simulation of climate when the orbital parameters of the earth with respect to the sun are changed (i.e., a numerical test of the Milankovitch hypothesis on the ice ages.)

In the second category, which concerns man's influence on climate, perhaps the most important use of the fully interactive ocean-atmosphere-biosphere model would be to study the changes in the entire climate system (including the changes in the stores of carbon in the ocean, atmosphere and biosphere) as a result of the burning of fossil hydrocarbons, or of man's modification of the living biomass (through desertification and deforestation, or conservation and afforestation.)

C. Notation

A_n	species dependent constants
c_p	specific heat of air (J kg^{-1} $°C^{-1}$) (≈ 1.01 at s.t.p.)
c_s	specific heat of soil (J m^{-3} $°C^{-1}$)
d	zero plane displacement (m)
$D_{h,\theta,vap}$	diffusivity of heat, water or vapor in the soil (m s^{-2})
$D[W_I]$	drainage rate (Kg m^{-2} s^{-1})
e_a	vapor pressure (mb)
e*	saturation vapor pressure (mb)
e_ℓ	vapor pressure in the substomatal cavity (mb)
E_I	interception loss rate (Kg m^{-2} s^{-1})
E_T	transpiration rate (kg m^{-2} s^{-1})
$f(\underline{e_a})$	vapor pressure component of stomatal resistance
$f(\underline{T_a})$	air temperature component of stomatal resistance
f(w)	scattering coefficient of canopy
$f(\beta)$	radiation extinction coefficient as a function of solar angle
$f(\psi_\ell)$	leaf water potential component of stomatal resistance
F_p	flow of water through the plant stem (Kg m^{-2} s^{-1} or mm hr^{-1})
$F_{p,crit}$	limiting value of F_p (Kg m^{-2} s^{-1})
g	acceleration due to gravity (m s^{-2})
G	heat flux to ground (W m^{-2})
h	height of the crop (m)
H	sensible heat flux to atmosphere (W m^{-2})
I_m	relative turbulence intensity
k	von Karman's constant (≈ 0.41)

$K_{m,v,h_{(z)}}$ conductivity of momentum, vapor and heat in the air ($m\ s^{-2}$)

K_T thermal conductivity of soil ($W\ m^{-2}\ °C^{-1}$)

K_θ hydraulic conductivity of soil ($m\ s^{-1}$)

$L_D(Z)$ leaf area density ($m^2\ m^{-3}$)

L_M local mixing length (m)

L_σ leaf area index ($m^2\ m^{-2}$)

n number of leaf layers

p throughfall coefficient

P rainfall rate ($kg\ m^{-2}\ s^{-1}$)

r radius (m)

r_a aerodynamic resistance ($s\ m^{-1}$)

r_{b_ℓ} leaf laminar boundary layer resistance ($s\ m^{-1}$)

r_{c_ℓ} canopy air space resistance ($s\ m^{-1}$)

r_c root cortex resistance (s)

$r_{c,o}$ root cortex resistance per unit length of root ($s\ m^{-1}$)

r_s soil resistance (s)

r_{st} stomatal resistance ($s\ m^{-1}$)

$r_{st}(\underline{S_a})$ component of stomatal resistance dependent on shortwave radiative intensity only ($s\ m^{-1}$)

r_x xylem resistance (s)

$r_{x,o}$ xylem resistance per unit height ($s\ m^{-1}$)

$R_{\underline{La}}$ longwave radiation incident on the surface ($W\ m^{-2}$)

R_N net radiation ($W\ m^{-2}$)

$RT_D(Z)$ root length density ($m\ m^{-3}$)

$\underline{S_a}$ solar radiation incident on surface ($W\ m^{-2}$)

$\underline{S_{a_{(o)}}}$ solar radiation incident above canopy ($W\ m^{-2}$)

$\underline{T_a}$ air temperature (°C)

T_b	temperature below which stomates close (°C)
T_d	deep soil temperature (°C)
T_ℓ	leaf temperature (°C)
T_o	temperature at which stomatal resistance factor, $f(\underline{T_a}) = 1$, (°C)
T_s	surface temperature (°C)
T_u	temperature above which stomates close (°C)
u	wind speed (m s^{-1})
U_R	flow of water through the plant root system (kg m^{-2} s^{-1} or mm hr^{-1})
W_ℓ	leaf water content (kg m^{-2} or mm)
W_I	water held on canopy surface (kg m^{-2} or mm)
z	height or depth (m)
z_b	height of bottom of canopy (m)
z_d	reference height (m)
z_ℓ	height of ℓth layer above ground (m)
z_m	height of leaf 'plate' (m)
z_o	roughness length (m)
z_T	height of top of canopy (m)
α	albedo
γ	psychrometric constant (mb $°C^{-1}$) = 0.646 at s.t.p.
λ	latent heat of vaporization (J kg^{-1}) = 2.501 at s.t.p.
ψ_ℓ	leaf water potential (bars)
ψ_r	root water potential (bars)
ψ_s	soil water potential (bars)
ρ	density of air (kg m^{-3}) (= 1.292 at s.t.p.)
θ	soil water content (kg m^{-3} or $m^3 m^{-3}$)
χ_s	leaf shape/shelter factor

D. References

Alfano, J. J., 1981: A Two-layer Ground Hydrology Model Interactive with an Atmospheric General Circulation Model. Ph.D. Thesis, University of Connecticut. 287 pp. and Appendices.

Allen, L. H. and Lemon, E. R., 1976: "Carbon Dioxide Exchange and Turbulence in a Costa Rica Tropical Rain Forest." In: Vegetation and the Atmosphere II; ed. by J. L. Monteith, pp. 265-308, Academic Press.

Atlas, D., and Thiele, O. T., 1981: "Precipitation Measurements from Space." Workshop Report, NASA, Goddard Space Flight Center, Greenbelt, Maryland 20771.

Beven, K. and Kirkby, M. J., 1976: "Towards a Simple, Physically-based, Variable Contributing Area Model of Catchment Hydrology." Leeds University, Department of Geography, Working Paper 154, 11 pp.

Calder, I. R. and Newson, M. D., 1979: "Land Use and Upland Water Resources in Britain - A Strategic Look." Water Resources Bulletin, American Water Resources Assoc., 15, pp. 1628-1639.

Camillo, P. J. and Schmugge, T. J., 1982: "A Computer Program for the Simulation of Heat and Moisture Flow in Soils." NASA Technical Memorandum 82121, Goddard Space Flight Center, Greenbelt, Maryland 20771.

Carson, D. J., 1981: "Current Parameterization of Land Surface Processes in Atmospheric General Circulation Models." In Proceedings of the JSC Study Conference on Land-Surface Processes in Atmosphere General Circulation Models, Greenbelt, USA, 5-10 January 1981.

Cowan, I. R., 1965: "Transport of Water in the Soil-Plant-Atmosphere System." J. Appl. Ecol., 2, pp. 221-239.

de Laubenfels, D. J., 1975: Mapping the World's Vegetation: Regionalization of Formations and Flora. Syracuse University Press. Syracuse, N.Y. 246 pp.

Denmead, O. T., 1976: "Temperate Cereals." In: Vegetation and the Atmosphere II. Ed. by J. L. Monteith, pp. 1-31, Academic Press.

Denmead, O. T. and Millar, B. D., 1976: "Water Transport in Plants (Wheat) in in the Field." Agron. J., 68, pp. 297-303.

Goudriaan, J., 1977: Crop Micrometeorology: A Simulation Study. Wageningen Center for Agricultural Publishing and Documentation. Wageningen, The Netherlands. pp.

Gurney, R. J. and Camillo, P. J., 1982: "Modelling Daily Evapotranspiration Using Remotely Sensed Data." NASA Technical Memorandum, (in press), Goddard Space Flight Center, Greenbelt, Maryland 20771.

Hillel, D., 1971: Soil and Water: Physical Principles and Processes. Academic Press, N.Y./San Francisco/London. 288 pp.

Hillel, D., 1977: "Computer Simulation of Soil-Water Dynamics: A Compendium of Recent Work." International Development Research Centre, Ottawa, Canada, pp. 214

Jarvis, P. G., 1976: "The Interpretation of the Variations in Leaf Water Potential and Stomatal Conductance found in Canopies in the Field." Phil. Trans. Roy. Soc. Lond. B. 273, pp. 593-610.

Leonard, R. E., and Eschner, A. R., 1968: "Albedo of Intercepted Snow." Water Resources Res., 4, pp. 931-935.

Loucks, O. L., Ek, A. R., Johnson, W. C. and Mouserud, R. A., 1981: "Growth, Aging and Succession." pp. 37-85 in Dynamic Properties of Forest Ecosystems, D. E. Reichle (ed.) Cambridge Univ. Press, Cambridge/London/N.Y. 683 pp. (International Biological Programme 23).

Male, D. H. and Granger, R. J., 1981: "Snow-Surface Energy Exchange. Water Resources Res., 17, pp 609-627.

Mintz, Y., 1979: "On the Simulation of the Oceanic General Circulation." In Report of the JOC Study Conference on Climate Models: Performance, Inter-Comparison and Sensitivity Studies, Washington, D.C., 3-7 April 1978. GARP Publication Series No. 22, Vol II, PP. 607-687. WMO, Geneva, 1979.

Mintz, Y., 1982: "The Sensitivity of Numerically Simulated Climates to Land-Surface Conditions." (Review paper presented at the JSC Study Conference on Land-Surface Processes in Atmospheric General Circulation Models, Greenbelt, USA, 5-10 January 1981. NASA Technical Memorandum 83985, Goddard Space Flight Center, 1982, 81 pp. [Will also appear in The Global Climate, J. Houghton, editor; Cambridge University Press, Cambridge/London/New York, 1983.]

Pinker, R.,1980: "The Microclimate of a Dry Tropical Forest." Agric. Meteor., 22, pp. 249-265.

Penning de Vries, F. W. T., 1971: "A Model for Simulating Transpiration of Leaves with Special Attention to Stomatal Functioning." J. Appl. Ecol., 9, pp. 57-77.

Raschke, K., 1975: "Stomatal action." Ann. Rev. Plant. Physiol., 26, pp. 309-340.

Ross, J. and Nilson, T. A., 1971: "A Mathematical Model of the Radiation Regime of Vegetation." In: V. K. Pyldmaa (Ed.) Actinometry and Atmospheric Optics, pp. 253-270.

Rutter, A. J., 1975: "The Hydrological Cycle in Vegetation." In Vegetation and the Atmosphere, Vol. 1, (ed. J. Monteith). Academic Press, London/New York/San Francisco. pp. 111-154.

Schmugge, T. J., Jackson, T. J. and McKim, H. L., 1980: "Survey of Methods for Soil Moisture Determination." Water Resources Research, 16, 6, pp 961-979.

Sellers, P. J., 1981: Vegetation Type and Catchment Water Balance: A Simulation Study. Ph.D. Thesis, Leeds University, Department of Geography, 836 pp.

Shukla, J. and Mintz, Y., 1982: "Influence of Land-Surface Evapotranspiration on the Earth's Climate." Science, 215, pp. 1498-1501.

Shuttleworth, W. J. and Calder, I. R., 1979: "Has the Priestley-Taylor Equation Any Relevance to Forest Evaporation?" J. Appl. Meteor., 18, pp. 639-646.

Thom, A. S., and Oliver, H. R., 1977: "On Penman's Equation for Estimating Regional Evaporation." Quart. J. Roy. Met. Soc., 101, pp. 93-105.

Turner, N. C., 1974: "Stomatal response to light and water under field conditions." Roy. Soc. N. Z. Bull. 12, pp. 423-432.